

Observation of $e^+e^- \rightarrow D_s^\pm D_s^{*\mp}$ at $\sqrt{s} = 4.14$ GeV

G. T. Blaylock, T. Bolton, J. S. Brown, K. O. Bunnell, T. H. Burnett, R. E. Cassell, D. Coffman, V. Cook, D. H. Coward, D. E. Dorfan, G. P. Dubois, G. Eigen, B. I. Eisenstein, T. Freese, G. Gladding, C. Grab, C. A. Heusch, D. G. Hitlin, J. M. Izen, L. Köpke, A. Li, W. S. Lockman, U. Mallik, C. G. Matthews, R. Mir, P. M. Mockett, R. F. Mozley, B. Nemati, A. Odian, J. Parker, L. Parrish, R. Partridge, D. Pitman, H. F. W. Sadrozinski, M. Scarlatella, T. L. Schalk, R. H. Schindler, A. Seiden, C. Simopoulos, I. E. Stockdale, W. Stockhausen, J. J. Thaler, W. Toki, B. Tripsas, F. Villa, S. Wasserbaech, A. Wattenberg, A. J. Weinstein, H. J. Willutzki, D. Wisinski, W. J. Wisniewski, R. Xu, and Y. Zhu

(The Mark III Collaboration)

California Institute of Technology, Pasadena, California 91125
 University of California at Santa Cruz, Santa Cruz, California 95064
 University of Illinois at Urbana-Champaign, Urbana, Illinois 61801
 Stanford Linear Accelerator Center, Stanford, California 94305
 University of Washington, Seattle, Washington 98195
 (Received 24 February 1987)

We present evidence for the exclusive reaction $e^+e^- \rightarrow D_s^\pm D_s^{*\mp}$, observed with the Mark III detector at the SLAC storage ring SPEAR. The D_s^\pm is reconstructed in the $\phi\pi^\pm$ decay mode, while the $D_s^{*\mp}$ is detected as a narrow peak in the recoil-mass distribution. The mass of the D_s^* is found to be $2109.3 \pm 2.1 \pm 3.1$ MeV/ c^2 , yielding a $D_s^*-D_s$ mass difference of $137.9 \pm 2.1 \pm 4.3$ MeV/ c^2 . The width of the D_s^* is < 22 MeV/ c^2 at the 90%-confidence level. The observed signal corresponds to $\sigma(e^+e^- \rightarrow D_s^+ D_s^{*-} + D_s^- D_s^{*+}) B(D_s^+ \rightarrow \phi\pi^+) = 30 \pm 6 \pm 11$ pb at $\sqrt{s} = 4.14$ GeV.

PACS numbers: 14.40.Jz, 13.25.+m, 13.65.+i

In the quark model, the lowest-lying $c\bar{s}$ pseudoscalar meson, the D_s^+ , has a higher-mass vector-meson partner, the D_s^{*+} .¹ In models with hyperfine corrections,² the D_s^{*+} mass is predicted to lie 80 to 150 MeV/ c^2 above that of the D_s^+ . Evidence has been presented for a narrow state decaying into a D_s^+ meson and a photon.^{3,4} Exclusive production of this state in association with the D_s in e^+e^- annihilation would provide new evidence that it is indeed the D_s^* . This Letter reports the first evidence of the exclusive reaction $e^+e^- \rightarrow D_s^\pm D_s^{*\mp}$, where the D_s^\pm is observed in the decay

$$D_s^+ \rightarrow \phi\pi^+ \quad (1)$$

or in the cascade

$$D_s^{*-} \rightarrow \gamma D_s^-, \quad D_s^- \rightarrow \phi\pi^-. \quad (2)$$

A precise measurement of the D_s^* mass is also reported.

The data sample represents an integrated luminosity of 6.30 ± 0.46 pb $^{-1}$ at $\sqrt{s} = 4.14$ GeV, collected with the Mark III detector at the SLAC storage ring SPEAR. A detailed description of the detector has been given elsewhere.⁵ Tracking information from the drift chamber, and time-of-flight (TOF) measurements from scintillation counters, are used in this analysis.

The analysis proceeds with the isolation of events containing one or more ϕ 's. A charged particle is identified as a kaon with use of TOF.⁶ The π - K separation is better than 5σ for kaons from reactions (1) and (2).⁷

Figure 1 shows the mass distribution of oppositely charged kaon pairs. The mass of a ϕ candidate is required to be within 10 MeV/ c^2 of the nominal ϕ mass. The $\phi\pi$ candidates are selected by the combining of a ϕ with each of the remaining charged tracks, assumed to be pions. A scatter plot of the $\phi\pi^+$ mass versus the recoil mass is shown in Fig. 2. Evidence for $D_s^+ D_s^{*-}$ production appears as a cluster of events near $M(\phi\pi^+) = 1.97$ GeV/ c^2 and $M(\text{recoil}) = 2.10$ GeV/ c^2 . Another cluster near $M(\phi\pi^+) = 1.87$ GeV/ c^2 and $M(\text{recoil}) = 2.01$ GeV/ c^2 is evidence for production of $D^+ D^{*-}$, with $D^+ \rightarrow \phi\pi^+$.⁸ Figure 3(a) shows the

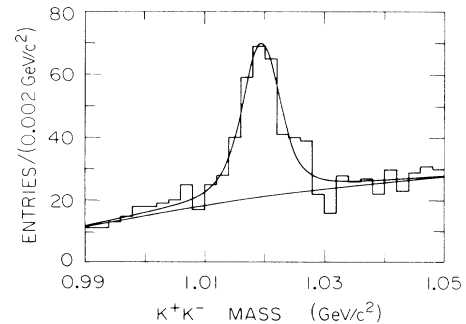
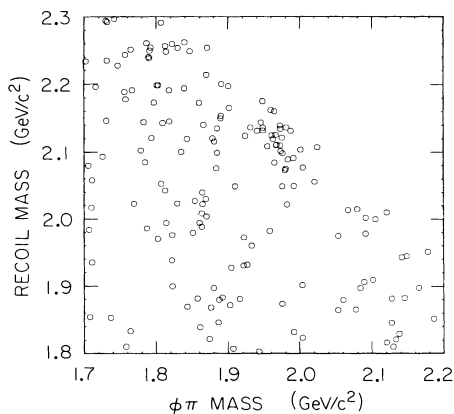


FIG. 1. The K^+K^- invariant-mass distribution. A fit to this distribution, with use of a Breit-Wigner line shape and a polynomial background, with $\Gamma(\phi) = 4.2$ MeV/ c^2 , yields $M(\phi) = 1019.3 \pm 0.4$ MeV/ c^2 , and $\sigma = 2.1 \pm 0.8$ MeV/ c^2 .

FIG. 2. Scatter plot of $M(\phi\pi^+)$ vs $M(\text{recoil})$.

recoil-mass distribution when the $\phi\pi^+$ mass is restricted to the D_s^+ region, 1.92 to 2.02 GeV/c^2 . This distribution contains the recoil from the D_s^+ 's produced in reactions (1) and (2). No significant evidence for $e^+e^- \rightarrow D_s^+D_s^-$, $D_s^+ \rightarrow \phi\pi^+$ is observed. The photon from the decay $D_s^{*+} \rightarrow \gamma D_s^+$ is not used in this analysis because of the limited energy resolution of the calorimeter. The D_s^* mass resolution would not be significantly improved, and the photon selection is ambiguous in events with many neutral showers.

The decay $D_s^+ \rightarrow \phi\pi^+$ is isolated by the requirement that the recoil mass lie between 2.04 and 2.18 GeV/c^2 [Fig. 3(b)]. An unbinned maximum-likelihood fit to this

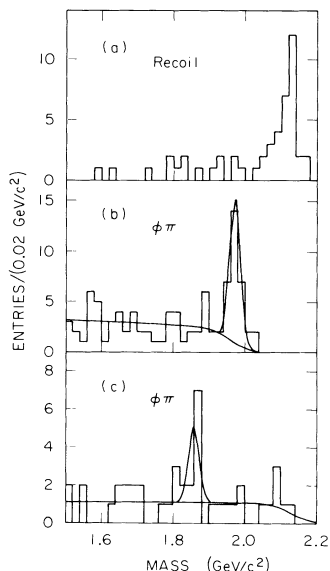


FIG. 3. (a) The projection of $M(\text{recoil})$ for $1.92 < M(\phi\pi^+) < 2.02 \text{ GeV}/c^2$. (b) The projection of $M(\phi\pi^+)$ for $2.04 < M(\text{recoil}) < 2.18 \text{ GeV}/c^2$. The fit is described in the text. (c) The projection of $M(\phi\pi^+)$ for $1.97 < M(\text{recoil}) < 2.05 \text{ GeV}/c^2$.

distribution with a Gaussian plus background yields 26.7 ± 5.2 (stat.) signal events above 5.6 background events. The fitted D_s^+ mass is $1972.4 \pm 3.7 \pm 3.7 \text{ MeV}/c^2$. The background shape is determined from the $\phi\pi^+$ mass distribution obtained by the combination of ϕ candidates with pions from different events. The mass resolution determined by Monte Carlo simulation ($\sigma = 15.1 \text{ MeV}/c^2$) is imposed in the fit. The systematic error includes variation of the selection criteria ($2.4 \text{ MeV}/c^2$), and uncertainties in the background shape ($2.5 \text{ MeV}/c^2$) and in the momentum scale⁹ ($1.1 \text{ MeV}/c^2$).

The analysis procedure and the absolute-mass scale are checked by investigating D decays in the data sample. The decay $D^+ \rightarrow \phi\pi^+$ is observed by the restricting of the recoil mass to the D^* mass region, 1.97 to 2.05 GeV/c^2 . The result is shown in Fig. 3(c): A fit with a Gaussian and a flat background yields a D^+ mass of $1860 \pm 7 \pm 4 \text{ MeV}/c^2$. The reactions $D^0 \rightarrow K^-\pi^+$, $D^0 \rightarrow K^-\pi^+\pi^-\pi^+$, and $D^+ \rightarrow K^-\pi^+\pi^+$ are analyzed with similar particle identification and recoil requirements, giving fitted masses of $1865.3 \pm 1.2 \text{ MeV}/c^2$, $1865.3 \pm 1.3 \text{ MeV}/c^2$, and $1870.6 \pm 2.6 \text{ MeV}/c^2$, respectively (statistical errors only).

To improve the D_s^* mass resolution, a D_s mass¹⁰ of $1971.4 \text{ MeV}/c^2$ is imposed as a constraint in the calculation of the recoil mass.¹¹ The resulting recoil-mass distribution (Fig. 4) shows a narrow peak at $2.11 \text{ GeV}/c^2$ from reaction (1), on a broad structure between 2.07 and 2.15 GeV/c^2 from reaction (2). A fit to this distribution yields

$$M(D_s^*) = 2109.3 \pm 2.1 \pm 3.1 \text{ MeV}/c^2.$$

The shape of the signal distribution and the resolution ($5.0 \text{ MeV}/c^2$) are determined from a Monte Carlo simulation which includes radiative corrections.¹² The background shape is determined from K^+K^- sidebands around the ϕ . The systematic error includes contributions from the uncertainties in the D_s^+ mass ($1.7 \text{ MeV}/c^2$), the center-of-mass energy at SPEAR (1.7

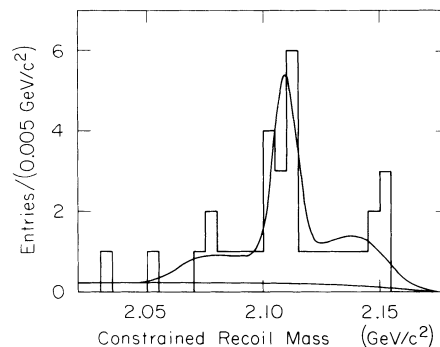


FIG. 4. The recoil-mass distribution with the D_s^+ mass constrained at $1971.4 \text{ MeV}/c^2$. The fit is described in the text.

MeV), the radiative corrections ($1.2 \text{ MeV}/c^2$), the selection criteria ($1.5 \text{ MeV}/c^2$), the background shape ($0.5 \text{ MeV}/c^2$), and the momentum scale ($0.1 \text{ MeV}/c^2$). The result implies¹³

$$M(D_s^*) - M(D_s) = 137.9 \pm 2.1 \pm 4.3 \text{ MeV}/c^2.$$

A maximum-likelihood calculation using the constrained recoil mass yields $\Gamma(D_s^*) < 22 \text{ MeV}/c^2$ at 90%-confidence level. The width and mass of the D_s^* are allowed to vary, while the resolution is fixed.

The decay angle distributions for the ϕ in the D_s^+ heli-

city frame, and the K^+ in the decay ϕ helicity frame are shown in Fig. 5. Since the D_s^+ helicity frame cannot be determined for the D_s^+ decays produced in reaction (2), all events are assumed to arise from reaction (1). For the hypothesis $J^P(D_s) = 0^-$ and $J^P(D_s^*) = 1^-$, the confidence levels of the $\cos\theta_\phi$ and $\cos\theta_{K^+}$ distributions with use of the Kolmogorov-Smirnov test¹⁴ are 0.62 and 0.39, respectively.

The production cross section times branching fraction is determined with the assumption of $B(D_s^{*+} \rightarrow \gamma D_s^+) = 100\%$. With use of the number of observed $D_s^+ \rightarrow \phi\pi^+$ decays (26.7 ± 5.2), and a $D_s^+ \rightarrow \phi\pi^+$ detection efficiency of 0.071, the result is

$$\sigma(e^+e^- \rightarrow D_s^+ D_s^{*-} + D_s^- D_s^{*+}) B(D_s^+ \rightarrow \phi\pi^+) = 30 \pm 6 \pm 11 \text{ pb}.$$

The systematic error includes contributions from the uncertainties in the detection efficiency (31%), the integrated luminosity (7%), and the background shape (15%). The contamination of the $\phi\pi^+$ sample by nonresonant $D_s^+ \rightarrow K^+ K^- \pi^+$ decays is negligible (< 0.5 events) for $B(D_s^+ \rightarrow K^+ K^- \pi^+) \simeq B(D_s^+ \rightarrow \phi\pi^+)$. The decay $D_s^+ \rightarrow \bar{K}^{*0} K^+ \rightarrow K^+ K^- \pi^+$ does not feed into the $\phi\pi^+$ sample because it is excluded by the ϕ requirement on the $K^+ K^-$ mass. This mode will be addressed in a future Mark III publication.

The measured $D_s^*-D_s$ mass difference can be compared with other vector-pseudoscalar splittings. For mesons containing at least one light quark, the mass-

squared difference, $\Delta_{M^2} = M^2(1^-) - M^2(0^-)$, is approximately constant.¹⁵ This effect has motivated calculations of the mass-squared difference within models which assume a simple confining potential.¹⁶ These models predict $\Delta_{M^2} \simeq 64\pi\alpha_s |\psi(0)|^2/9\mu$, where $\psi(0)$ is the wave function at the origin and μ is the reduced mass of the quarks. An approximately constant mass-squared difference follows for specific choices of α_s and the form of the potential.¹⁶ Our measurement of the $D_s^*-D_s$ mass difference results in $\Delta_{M^2} = 0.563 \pm 0.020 \text{ (GeV}/c^2)^2$, which is consistent with this empirical rule.

In summary, the exclusive reaction $e^+e^- \rightarrow D_s^+ D_s^{*-}$ at $\sqrt{s} = 4.14 \text{ GeV}$ is observed. The production cross section times branching fraction and the D_s^* mass are measured. The decay angular distributions are consistent with those expected for a pseudoscalar D_s and a vector D_s^* . These results are in good agreement with previous measurements of the D_s ¹⁷ and the D_s^* .⁴

We gratefully acknowledge the dedicated efforts of the SLAC storage ring SPEAR staff and we also thank Dr. G. Fischer for many conversations concerning the SPEAR energy calibration. One of us (G.E.) wishes to thank the A. von Humboldt Foundation for support. This work was supported by the U.S. Department of Energy, under Contracts No. DE-AC03-76SF00515, No. DE-AC02-76ER01195, No. DE-AC03-81ER40050, and No. DE-AM03-76SF00034 and by the National Science Foundation.

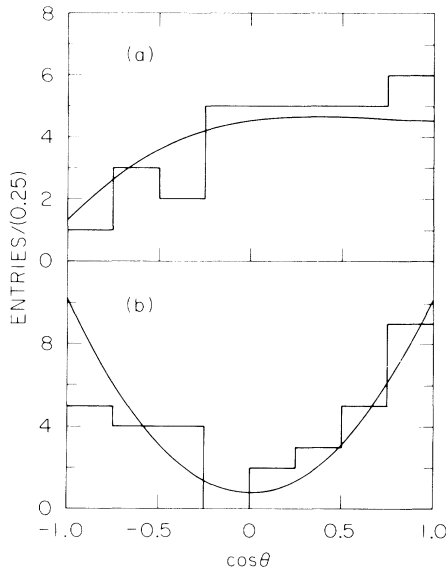


FIG. 5. (a) The $\cos\theta_\phi$ distribution in the D_s^+ helicity frame. (b) The $\cos\theta_{K^+}$ distribution in the ϕ helicity frame. The data are not acceptance corrected. The curves show the distributions from a Monte Carlo simulation which includes equal amounts of reactions (1) and (2), plus 18% background as determined from the fit to Fig. 3(b).

¹The D_s^+ and D_s^{*+} were formerly denoted the F^+ and F^{*+} , respectively. Throughout this paper we adopt the convention that reference to a state also implies reference to its charge conjugate.

²For a recent discussion see S. Godfrey and N. Isgur, Phys. Rev. D **32**, 189 (1985), and references therein.

³The first evidence for the D_s^{*+} was reported by R. Brandelik *et al.*, Phys. Lett. **70B**, 132 (1977), and R. Brandelik *et al.*, Phys. Lett. **80B**, 412 (1979). These measurements were not confirmed by R. Partridge *et al.*, Phys. Rev. Lett. **47**, 760

(1981), and R. P. Horisberger, Ph.D. thesis, SLAC Report No. 266, 1984 (unpublished).

⁴H. Aihara *et al.*, Phys. Rev. Lett. **53**, 2465 (1984); H. Albrecht *et al.*, Phys. Lett. **146B**, 111 (1984).

⁵D. Bernstein *et al.*, Nucl. Instrum. Methods Phys. Res., Sect. A **226**, 301 (1984).

⁶The charged-kaon tracks are required to have $|(t_K^p - t^m)/\sigma_K| < |(t_K^p - t^m)/\sigma\pi|$, where t_K^p (t_K^m) is the predicted TOF for a kaon (π) mass hypothesis, t^m is the measured TOF, and σ_K (σ_π) is the TOF error for the kaon (π) mass hypothesis.

⁷In the Monte Carlo simulation, the D_s and D_s^* are assumed to be pseudoscalar and vector, respectively, with $B(D_s^* \rightarrow \gamma D_s) = 100\%$.

⁸The Cabibbo-suppressed decay $D^+ \rightarrow \phi\pi^+$ has been observed by R. Bailey *et al.*, Phys. Lett. **139B**, 320 (1984), and R. M. Baltrusaitis *et al.*, Phys. Rev. Lett. **55**, 150 (1985).

⁹The uncertainty in the absolute momentum scale, $\sigma(p)/p = 0.1\%$, has been estimated with use of the following reactions: $e^+e^- \rightarrow \mu^+\mu^-$; $K_S^0 \rightarrow \pi^+\pi^-$; $J/\psi \rightarrow p\bar{p}$; $D^0 \rightarrow K^-\pi^+$, $K^-\pi^+\pi^+\pi^-$; and $D^+ \rightarrow K^-\pi^+\pi^+$.

¹⁰A weighted average of $M(D_s^+) = 1971.4 \pm 1.7$ MeV/ c^2 is obtained with use of the measurements tabulated in M. Aguilar-Benitez *et al.* (Particle Data Group), Phys. Lett.

170B, 1 (1986), replacing the previous Amsterdam-Bristol-CERN-Cracow-Munich-Rutherford (ACCMOR) value with their later measurement, $M(D_s^+) = 1972.7 \pm 1.5 \pm 1.0$ MeV/ c^2 ; H. Becker *et al.*, CERN Report No. CERN-EP/86-172, 1986 (to be published).

¹¹ $M(\text{recoil}) = (\{\sqrt{s} - [M^2(D_s) + p^2(D_s)]^{1/2}\}^2 - p^2(D_s))^{1/2}$, where $M(D_s)$ is fixed.

¹²Only initial state radiation is considered with use of a method from F. Behrends and R. Kleiss, Nucl. Phys. **B178**, 141 (1981).

¹³For $e^+e^- \rightarrow D_s^* D_s$ at $\sqrt{s} = 4.14$ GeV, $\delta M(D_s^*) \cong -\delta M(D_s)$. The systematic errors are $\sigma[M(D_s^*)] = \{(2.6 \text{ MeV}/c^2)^2 + \sigma^2[M(D_s)]\}^{1/2}$ and $\sigma[M(D_s^*) - M(D_s)] = \{(2.6 \text{ MeV}/c^2)^2 + 4\sigma^2[M(D_s)]\}^{1/2}$.

¹⁴D. B. Owen, *Handbook of Statistical Tables* (Addison-Wesley, Reading, MA, 1962).

¹⁵ $\Delta_{M^2} = 0.575$ (GeV/ c^2)² for $\rho^0 - \pi^0$, 0.556 (GeV/ c^2)² for $K^{*0} - K^0$, and 0.551 (GeV/ c^2)² for $D^{*0} - D^0$. For a discussion of the empirical relation see A. Martin, Comments Nucl. Part. Phys. **16**, 249 (1986).

¹⁶K. Igi and S. Ono, Phys. Rev. D **32**, 232 (1985); M. Frank and P. O'Donnell, CERN Report No. CERN-TH-4367/86, 1986 (to be published).

¹⁷M. Aguilar-Benitez *et al.*, in Ref. 10.